# Single channel properties of hyperpolarization-activated cation currents in acutely dissociated rat hippocampal neurones

T. A. Simeone[1,2], J. M. Rho[2] and T. Z. Baram[1]

[1] *Departments of Anatomy & Neurobiology and Pediatrics, University of California at Irvine, Irvine, CA, USA*
[2] *Barrow Neurological Institute and St Joseph's Hospital & Medical Center, Phoenix, AZ, USA*

**The hyperpolarization-activated cation current ($I_h$), mediated by HCN channels, contributes to intrinsic neuronal properties, synaptic integration and network rhythmicity. Recent studies have implicated HCN channels in neuropathological conditions including epilepsy. While native HCN channels have been studied at the macroscopic level, the biophysical characteristics of individual neuronal HCN channels have not been described. We characterize, for the first time, single HCN currents of excised inside-out patches from somata of acutely dissociated rat hippocampal CA1 pyramidal cells. Hyperpolarization steps elicited non-inactivating channel openings with an apparent conductance of 9.7 pS, consistent with recent reports of native and recombinant HCN channels. The voltage-dependent $P_o$ had a $V_{1/2}$ of $-81 \pm 1.8$ mV and slope $-13.3 \pm 1.9$ mV. Blockers of macroscopic $I_h$, ZD7288 (50 $\mu$M) and CsCl (1 mM), reduced the channel conductance to 8 pS and 8.4 pS, respectively. ZD7288 was slightly more effective in reducing the $P_o$ at depolarized potentials, whereas CsCl was more efficacious at hyperpolarized potentials. The unitary neuronal HCN channels had voltage-dependent latencies to first channel opening and two open states. As expected, ZD7288 and CsCl increased latencies and decreased the properties of both open states. The major endogenous positive modulator of macroscopic $I_h$ is cAMP. Application of 8Br-cAMP (10 $\mu$M) did not affect conductance (9.4 pS), but did increase $P_o$ and short and long open times. Thus, sensitivity to $I_h$ modulators supports the single h-channel identity of these unitary currents. Detailed biophysical analysis of unitary $I_h$ conductances is likely to help distinguish between homomeric and heteromeric expression of these channels – findings that may be relevant toward the pathophysiology of diseases such as epilepsy.**

(Resubmitted 21 June 2005; accepted after revision 4 August 2005; first published online 25 August 2005)
**Corresponding author** T. Z. Baram: University of California, Irvine, Anatomy and Neurobiology, Med Sci I, Rm B-151, ZOT: 4475, Irvine, CA 92697, USA. Email: tallie@uci.edu

The hyperpolarization-activated cation current ($I_h$) contributes to intrinsic membrane properties as well as network responses of neurones (Accili *et al.* 2002; Robinson & Siegelbaum, 2003; Santoro & Baram, 2003; Poolos, 2004). Transmembrane hyperpolarization below $-40$ mV activates $I_h$, producing a depolarizing current carried by $Na^+$ and $K^+$ ions. In addition to its established role in pacemaker activity, $I_h$ contributes to the properties of non-pacemaking neurones. In specific cell types $I_h$ is involved in control of resting membrane potential and of membrane resistance (Lupica *et al.* 2001; Surges *et al.* 2004). $I_h$ impacts on the shape and propagation of subthreshold voltage potentials in dendrites, modulating integration of synaptic inputs (Magee, 1998, 1999; Santoro & Baram, 2003; Poolos, 2004), and contributes to the regulation of synaptic transmission (Beaumont & Zucker, 2000; Lupica *et al.* 2001; van Welie *et al.* 2004).

A family of ion channel subunits termed the hyperpolarization-activated cyclic-nucleotide gated (HCN) channels has been identified as the molecular correlates of $I_h$ (Santoro *et al.* 2000). The four members of the HCN family have been heterologously expressed and their activation results in current properties similar to native $I_h$. However, each HCN isoform exhibits distinct properties. For example, HCN1 channels have faster kinetics and reduced sensitivity to cAMP compared to HCN2 or HCN4 channels. In the central nervous system, differential regional distribution and developmental expression patterns distinguish the HCN channel isoforms, suggesting specialized functional roles across

 DOI: 10.1113/jphysiol.2005.093161

space and time (Bender *et al.* 2001; Vasilyev & Barish, 2002).

The increasingly evident contribution of h-channels to both normal and neuropathological neuronal function has led to their intense investigation. These studies have relied on the properties of whole-cell $I_h$, limiting a full understanding of channel behaviour. Single h-channels have been recorded in dissociated sinoatrial node cells (DiFrancesco, 1986; DiFrancesco & Mangoni, 1994) and in cardiac myocytes (Michels *et al.* 2005) where their conductance ranged from ~1 to ~19 pS. However, the properties of single h-channel currents in neurones have not been reported. Here we describe and characterize single h-channels recorded in dissociated CA1 hippocampal neurones. These non-inactivating channels are progressively activated by hyperpolarization, enhanced by 8Br-cAMP, and blocked by ZD7288 and CsCl.

## Methods

### Preparation

CA1 pyramidal neurones were acutely dissociated from hippocampal slices prepared from postnatal day (P)10–22 Sprague-Dawley rats, using procedures modified from Kay & Wong (1986). Briefly, rats were decapitated without anaesthesia, and brains were quickly removed and placed in ice cold PIPES saline bubbled with 95% $O_2$–5% $CO_2$. Pipes saline contained (mM): 120 NaCl, 5 KCl, 1 $CaCl_2$, 1 $MgCl_2$, 25 D-glucose and 20 Pipes (pH 7.0). Coronal sections (600 $\mu$m) were prepared with a Vibratome 1000 Plus (Vibratome). The hippocampal CA1 subfield was microdissected and incubated in Pipes saline with Protease XXIII (3 mg ml$^{-1}$; Sigma) at 30°C for 15 min. CA1 regions were transferred to 22–23°C Pipes saline under moderate stirring for 1 h. Cells were dispersed in poly L-lysine (Sigma) coated 35 mm culture dishes by gentle trituration with fire-polished Pasteur pipettes of descending bore diameters and allowed to settle for $>$ 15 min before recording. All procedures involving animals were in accordance with National Institutes of Health guidelines and were approved by the University of California at Irvine Institutional Care and Use Committee.

### Electrophysiology

Unitary h-channel currents were recorded in excised inside-out patches according to previously established techniques (Hamill *et al.* 1981; Rho *et al.* 1996). Briefly, pyramidal cells were identified by the presence of a relatively long apical dendrite, pyramidal soma, and basal processes. The composition of the bath solution was (mM): 100 potassium gluconate, 50 KCl, 4 NaCl, 1 $CaCl_2$, 5 EGTA, and 10 HEPES (adjusted to pH 7.25 with KOH and to 320–325 mosmol l$^{-1}$ with sucrose). The pipette filling solution contained (mM): 140 NaCl, 5 KCl, 2 $CaCl_2$, 1 $MgCl_2$ and 10 Hepes (pH 7.4 with NaOH; 310–315 mosmol l$^{-1}$). Pipette solutions contained blockers of voltage- and ligand-gated channels, including tetrodotoxin (TTX, 1 $\mu$M), tetraethylammonium chloride (TEA, 10 mM), $BaCl_2$ (1 mM), $CdCl_2$ (0.2 mM), picrotoxin (10 $\mu$M), 6,7-dinitroquinoxaline-2,3-(1H,4H)-dione (DNQX, 10 $\mu$M), and D(−)-2-amino-5-phosphonopentanoic acid (APV, 20 $\mu$M). To confirm the identity of the channels, ZD7288 (50 $\mu$M; Tocris) was added to the bath solution, or CsCl (1 mM) or 8-bromo-adenosine 3′,5′-cyclic monophosphate (8Br-cAMP, 10 $\mu$M) was added to the pipette solution.

Recording pipettes were prepared from borosilicate glass capillaries (VWR) coated with Sylgard (Dow Corning Corp.) and fire-polished (Narishige) to final resistances of 5–9 MΩ. Only patches with seal resistances $\geq$ 20 GΩ were included in the analysis. Single-channel currents were recorded at room temperature (22–23°C) using a Multiclamp 700A and pCLAMP9.0 software (Axon Instruments, Union City, CA, USA). Signals were acquired at 20 kHz and filtered at 1 kHz (−3 dB, 4-pole Bessel). Inside-out patches, pulled from the soma and held at a transmembrane potential of −30 mV, were hyperpolarized in 5 or 10 mV steps. At least ten 2.5 s steps to a single voltage were sequentially recorded before moving onto the next hyperpolarizing voltage. There was 8 s between the start of each step.

### Data analysis

Signals were subjected to *post hoc* Gaussian (1 kHz) and electrical interference filtering. Leak and capacitive currents were averaged in null sweeps or segmented averages of sweeps and then subtracted from records with channel openings (Clampfit 9.0, Axon Instruments). Events were detected using a conventional 50% threshold level criterion under direct surveillance of event detection interpretation (without automation). Events shorter than or equal to the dead time of our system (0.2 ms) were excluded and, owing to uncertainty of duration, openings or closings persisting at the end of command pulses were not included in dwell-time analysis. Mean open times were determined from conventional histograms fitted with standard exponential equations and the first bin was rejected prior to curve fitting to reduce distortion due to false or missing events. It should be noted that time constants of less than 1 ms were at the limit of filter resolution, so that further dissection of the gating processes was not attempted. Current amplitudes were calculated

from amplitude histograms fitted with a Gaussian equation. Latency to first channel opening was analysed with cumulative distribution histograms. Gaussian and exponential fitting used Levenberg-Marquardt search methods (Clampfit 9.0).

Raw open probabilities were calculated as the percentage of the time a channel was open during a 2.5 s voltage step (Clampfit 9.0). The $P_o$ data was fitted with a Boltzmann equation of form $P_o = P_{o(max)}/\{1 + \exp[V_m - V_{1/2}]/s\}$, where $P_{o(max)}$ is the maximal open probability, $V_{1/2}$ is the voltage of half-maximal $P_o$, and $s$ is the constant slope factor. Current–voltage ($I$–$V$) plots were constructed and linear regression performed using GraphPad Prism 4.0 software (GraphPad Software Inc., San Diego, CA, USA). Ionic permeability ratios were calculated using the equation:

$$E_{rev} = (RT/F)\ln\{[K_o + (P_{Na}/P_K)Na_o]/[K_i + (P_{Na}/P_K)Na_i]\},$$

where $E_{rev}$ is the reversal potential, $P_{Na}$ and $P_K$ are $Na^+$ and $K^+$ permeability, $K_i$ and $Na_i$ are the internal (bath) $K^+$ and $Na^+$ concentrations, $K_o$ and $Na_o$ are the external (pipette) $K^+$ and $Na^+$ concentrations, $F$ is the Faraday constant, $R$ is the universal gas constant, and $T$ is absolute temperature.

## Results

### Hyperpolarization elicits single channel openings with properties consistent with macroscopic h-currents

Inside-out patches were excised from somata of acutely dissociated CA1 pyramidal cells. Apparent duration and amplitude of channel openings increased as a function of hyperpolarization (Fig. 1*A*). Consecutive steps (2.5 s) from −30 mV to −70 mV illustrate the various latencies and opening probabilities observed among traces (Fig. 1*B*). The ensemble average of 152 traces of −70 mV steps

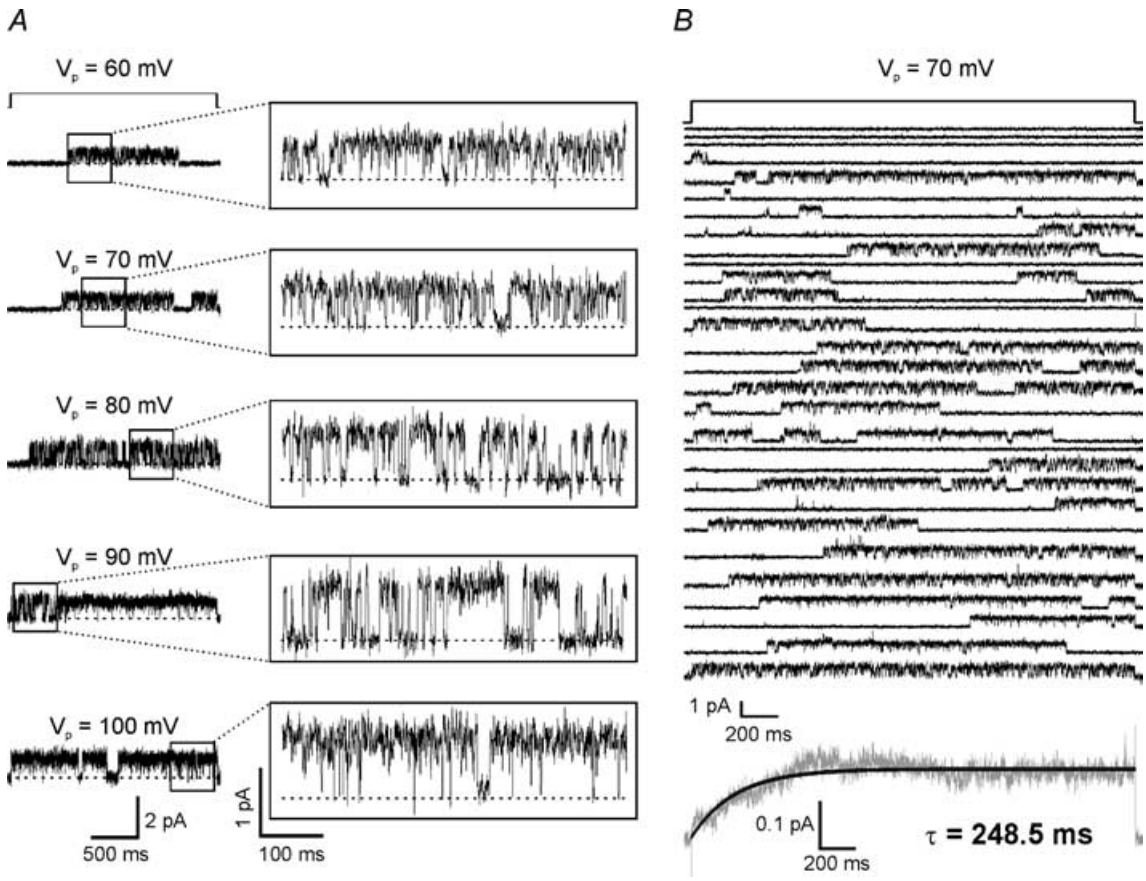


**Figure 1. Hyperpolarization elicits single-channel openings**
*A*, single h-channel currents obtained at five hyperpolarizing voltage command steps from an inside-out patch held at $V_p = 30$ mV. The dashed line indicates the closed state. *B*, top, 30 representative traces of 2.5 s steps from $V_p = 30$ mV to 70 mV from an individual patch. Bottom, ensemble average current of 152 traces of steps to 70 mV ($n = 8$ patches) reveals a slowly activating current that can be fitted with a single exponential equation (black line). Given the limitations of our recording system, we excluded traces with latencies of less than 1 ms from the ensemble average ($n = 49$ traces). Based on inside-out patch configuration, positive (upward) deflections represent inward current.

demonstrated a slowly activating current that was fitted with a single exponential equation ($\tau = 248.5 \pm 1.4$, mean ± s.e.m., $r = 0.87$, $n = 8$ patches; Fig. 1*B*, bottom).

Raw open probabilities ($P_o$) were voltage dependent, increasing from 0.16 at −60 mV to 0.79 at −120 mV (Fig. 2*A*). The channel $P_o$ had a $V_{1/2}$ of $-81.3 \pm 1.8$ mV and slope of $-13.3 \pm 1.9$ mV (Boltzmann fit ± s.e.m.), similar to macroscopic $I_h$ values. Mean current amplitudes of individual patches calculated from Gaussian fits of amplitude histograms were plotted *versus* voltage to examine the current–voltage (*I–V*) relationship of channel openings (Fig. 2*B*). The extrapolated reversal potential, calculated by linear regression, was −8.1 mV, with a slope conductance of 9.7 pS. This reversal potential approximated previous cell-attached and inside-out patch experiments (DiFrancesco, 1986; DiFrancesco & Mangoni, 1994).

The mean latency time to the first channel opening decreased with hyperpolarization (e.g. $518 \pm 125$ ms at −60 mV and $41 \pm 26$ ms at −100 mV; Fig. 2*C*). Cumulative distribution histograms further demonstrated the voltage dependence of these latencies (Fig. 2*D*) and illustrate that 66% of the 2.5 s steps to −60 mV evoked channel openings, *versus* 100% of steps to −100 mV.

Hyperpolarization also affected mean open times of the unitary currents. Channel open time histograms were best fitted with double exponential equations, indicating that the channels had at least two open states (Table 1). The long

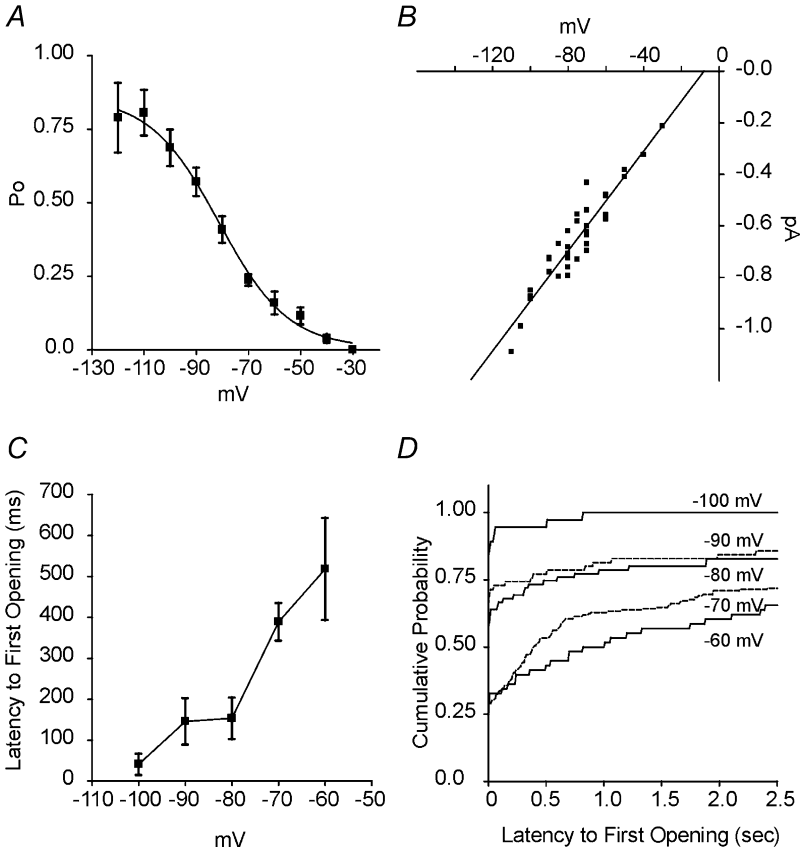


**Figure 2. Properties of single-channels are voltage dependent**
*A*, $P_o$ values increased with incremental hyperpolarization steps and had a half-activation voltage of −81.3 mV and a slope of e-fold change for −13.3 mV, calculated with a Boltzmann equation ($r = 0.997$; $n = 40$–201 sweeps from 5 to 8 patches, except for −110 and −120 mV where $n = 10$ sweeps from 1 patch). *B*, the *I–V* relationship of the single-channel currents indicates a mixed ionic permeability of the channel. Linear regression of the *I–V* data gave a reversal potential of −8.1 mV and conductance of 9.7 pS ($r = 0.95$). Similarly, Gaussian-fit histograms of pooled events from all patches (not shown) resulted in current amplitudes of $-0.21 \pm 0.004$, $-0.33 \pm 0.04$, $-0.39 \pm 0.07$, $-0.52 \pm 0.11$, $-0.63 \pm 0.2$, $-0.71 \pm 0.12$, $-0.77 \pm 0.06$, $-0.85 \pm 0.16$, $-0.97 \pm 0.03$ and $-1.1 \pm 0.15$ pA at −30, −40, −50, −60, −70, −80, −90, −100, −110 and −120 mV, respectively, giving a conductance of 9.5 pS (Gaussian mean ± s.d.; slope conductance found by linear regression, $r = 0.997$). *C*, averaged latencies to first channel openings after a voltage step, decreased with hyperpolarization. Only steps activating channels were included ($n = 35$–151 sweeps from 5 to 8 patches). *D*, cumulative frequency distribution histograms demonstrated the voltage-dependence of latency to first opening for the channels (bin width = 10 ms). Sweeps with no channel openings were included ($n = 40$–201 sweeps from 5 to 8 patches). Voltages and current amplitudes are corrected for patch configuration.

and short open time constants ($\tau_{long}$ and $\tau_{short}$) increased with hyperpolarization from 6 ms to 30 ms and 1.8 ms to 3.2 ms between −60 mV and −100 mV, respectively.

The number of functional channels in the soma–proximal dendrite compartment of CA1 pyramidal cells was estimated using mean current density (∼3.3 pA pF$^{-1}$) and mean whole-cell capacitance (∼135 pF) values reported by Vasilyev & Barish (2002) obtained at −120 mV from cells of P20 mice at 22–24°C (Vasilyev & Barish, 2002). Utilizing the equation $I = Npi$ (Hille, 2001), where $I$ is the macroscopic whole cell current calculated from the above current density and capacitance, $N$ is the number of channels, $p$ is the single channel $P_o$ and $i$ is the mean unitary current amplitude at −120 mV, it is estimated that the soma–proximal dendrites contain ∼513 h-channels. A second estimation was calculated using the mean macroscopic conductance (∼4.7 nS) also reported by Vasilyev & Barish (2002). A similar equation, $G = Np\gamma$ (Johnston & Wu, 1995), where $G$ is the mean macroscopic conductance, $p$ is the single channel $P_o$ at −120 mV, and $\gamma$ is the mean unitary conductance, estimated ∼623 h-channels. However, both of these channel estimates are slight overestimates because Vasilyev & Barish (2002) used an external 10 mM $K^+$ solution, whereas 5 mM $K^+$ was used in the present experiments. Assuming a specific membrane capacitance of $10^{-2}$ pF $\mu$m$^{-2}$ (Hille, 2001), the above mean whole-cell capacitance yields a soma–proximal dendrite surface area of 13 500 $\mu$m$^2$ and channel density of ∼0.04 channels $\mu$m$^{-2}$. According to Magee (1998), distal dendritic $I_h$ density increases 10-fold compared to soma (i.e. ∼0.4 channels $\mu$m$^{-2}$). Similar values result using Magee's (1998) conductance density measurements from CA1 pyramidal cells of > P35 rats under physiological conditions (soma: 1–2 pS $\mu$m$^{-2}$; dendrite: 8–10 pS $\mu$m$^{-2}$) yielding somatic and dendritic densities of ∼0.1 channels $\mu$m$^{-2}$ and ∼1 channel $\mu$m$^{-2}$, respectively.

## Hyperpolarization-evoked single channels are inhibited by ZD7288 and CsCl

Patches were exposed to the specific, internal $I_h$ blocker ZD7288 (50 $\mu$M; bath-applied) or to the external blocker CsCl (1 mM; included in the pipette solution) (Fig. 3*A*). The $P_o$ of the unitary currents was reduced by these blockers of macroscopic $I_h$: e.g. ZD7288 reduced $P_o$ by 90%, 62%, 54%, 54%, and 82% at −60, −70, −80, −90, and −100 mV, whereas CsCl decreased $P_o$ by 15%, 24%, 89%, 96%, 84%, 88% and 93% at −50, −60, −70, −80, −90, −100 and −120 mV, respectively (Fig. 3*B*). Also, latency to first channel opening was increased, and the cumulative probability of first opening by 500 ms after a −70 mV step was 0.53 in control conditions, but only 0.2 and 0.08 in ZD and CsCl, respectively (Fig. 3*C*). The extrapolated reversal potentials of the channels in ZD7288- and CsCl-exposed patches were −4.2 mV and −5.5 mV with slope conductances of 8.0 pS and 8.4 pS, respectively (Fig. 3*D*). Similar to an apparent $P_{Na}/P_K$ of 0.76 in control conditions, the apparent channel $P_{Na}/P_K$ values in ZD7288 and CsCl were 0.89 and 0.85, respectively.

**Table 1. Open time constants**

| mV | $\tau_{long}$ (ms) | $A_{long}$ | $\tau_{short}$ (ms) | $A_{short}$ | $r$ | $n$ | Events |
|---|---|---|---|---|---|---|---|
| Control | | | | | | | |
| −60 | 5.8 | 66% | 1.8 | 34% | 0.97 | 6 | 8768 |
| −70 | 10.5 | 39% | 2.3 | 61% | 0.97 | 8 | 17353 |
| −80 | 16.8 | 12% | 3.2 | 88% | 0.96 | 8 | 5350 |
| −90 | 19.3 | 23% | 3.0 | 77% | 0.91 | 6 | 3924 |
| −100 | 30.0 | 12% | 3.2 | 88% | 0.91 | 5 | 2052 |
| ZD7288 (50 $\mu$M) | | | | | | | |
| −60 | 17.5* | 7%* | 1.8 | 93%* | 0.96 | 3 | 3208 |
| −70 | 14.5† | 9%* | 1.9* | 91%* | 0.97 | 6 | 7714 |
| −80 | 16.8 | 8%* | 1.5* | 92%* | 0.97 | 9 | 7695 |
| −90 | 12.8* | 12%* | 1.3* | 88%* | 0.94 | 7 | 6069 |
| −100 | 13.4* | 19%* | 1.0* | 81%* | 0.90 | 2 | 1387 |
| CsCl (1 mM) | | | | | | | |
| −60 | n.d. | | n.d. | | | | |
| −70 | 6.6* | 20%* | 0.8* | 80%* | 0.91 | 4 | 1695 |
| −80 | 1.7* | 41%* | 0.4* | 59%* | 0.96 | 1 | 2712 |
| −90 | 1.2* | 48%* | 0.4* | 52%* | 0.98 | 1 | 5036 |
| −100 | n.d. | | n.d. | | | | |

Open times were calculated from standard exponential fits of distribution histograms (bin width = 1 ms for control and ZD7288; bin width = 0.5 ms for CsCl). Abbreviations: $\tau$, time constant; $A$, area that $\tau_{long}$ or $\tau_{short}$ contributes to the exponential fit; $r$, correlation coefficient of exponential fit; $n$, number of patches; n.d., not determined. Voltages corrected for patch configuration. Significance was determined with unpaired $t$ tests. *$P \leq 0.001$, †$P \leq 0.01$ *versus* control patches.

Channel open times (long and short) were also reduced by ZD7288 and CsCl (Table 1). Interestingly, ZD7288 decreased $\tau_{long}$ at potentials more hyperpolarized than −80 mV, but increased $\tau_{long}$ at potentials more depolarized than −80 mV. However, ZD7288 significantly decreased the contribution of $\tau_{long}$ to the exponential fit at potentials more depolarized than −80 mV. This indicates that, though the channels had prolonged $\tau_{long}$ values, they entered this open state less frequently. ZD2788 reduced $\tau_{short}$ at potentials more hyperpolarized than −70 mV. CsCl decreased both $\tau_{long}$ and $\tau_{short}$, with a greater effect at hyperpolarized potentials. The marked inhibition of the single channel currents by putative blockers of macroscopic $I_h$ strongly supports the identification of these channels as h-channels.

## Hyperpolarization-evoked single channels are potentiated by 8Br-cAMP

Macroscopic $I_h$ is enhanced by direct interaction with cAMP. Therefore, patches were exposed to the

membrane-permeant 8Br-cAMP (10 $\mu$M; included in the pipette solution) (Fig. 4*A*). Interestingly, unitary currents were observed at −30 mV in 3/6 patches, and by −60 mV all patches exhibited channel openings. 8Br-cAMP increased the raw $P_o$ at all voltages; however, for unknown reasons, every patch was lost by −90 mV and the $P_o$–$V$ curve did not plateau (Fig. 4*B*). In previous studies, cAMP and forskolin, an adenylate cyclase activator, did

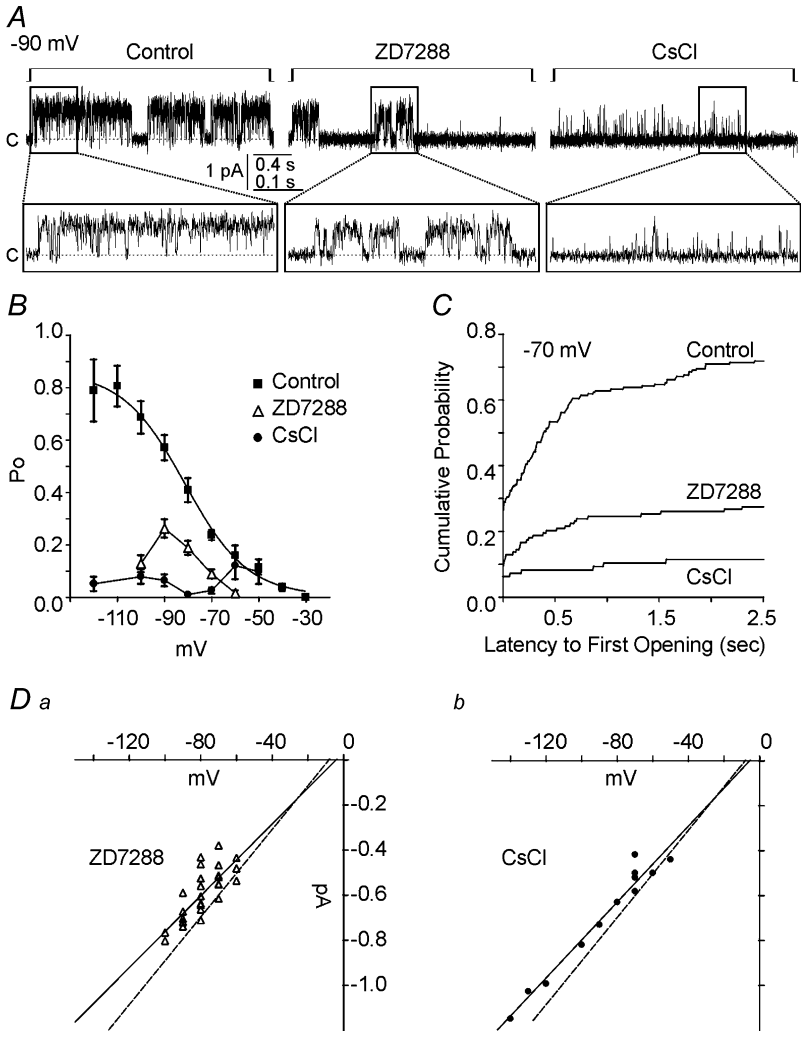


**Figure 3. $I_h$ blockers decrease open probabilities, increase first-latencies and slightly decrease conductance of single h-channels**

*A*, representative traces of channel openings elicited by hyperpolarization steps from −30 mV to −90 mV in control, 50 $\mu$M ZD7288 and 1 mM CsCl conditions. Based on inside-out patch configuration, positive (upward) deflections represent inward current. Closed state is indicated by c and dashed line. *B*, ZD7288 (50 $\mu$M) reduced $P_o$s in an apparent voltage-dependent manner with greatest inhibition at depolarized potentials. In contrast, inhibition by CsCl (1 mM) was greatest at hyperpolarized potentials. (ZD7288 bath applied: $n = 65$–168 sweeps from 7 to 14 patches; CsCl included in the pipette solution: $n = 38$–96 sweeps from 4 to 10 patches.) *C*, cumulative frequency distribution histograms of the latency to first channel openings during a −70 mV step demonstrated the dramatic increases in latencies caused by 50 $\mu$M ZD7288 and 1 mM CsCl (bin width = 10 ms). Sweeps with no channel openings were included (control, $n = 201$ sweeps from 8 patches; ZD7288, $n = 137$ sweeps from 14 patches; CsCl, $n = 96$ sweeps from 10 patches). *D*, ZD7288 and CsCl slightly reduced the channel conductance to 8.0 and 8.4 pS ($r = 0.78$ and 0.98), respectively. Dashed line is the control *I–V* fit from Fig. 2. Voltages and current amplitudes are corrected for patch configuration. Compared to control patches (Fig. 2 legend), the amplitude histograms of pooled events from all inhibitor-exposed patches that did have openings had lower Gaussian means at all voltage steps, but were not significantly different from control ($P > 0.05$; unpaired *t* test). Channel openings of ZD7288-exposed patches had mean amplitudes of $-0.43 \pm 0.07$, $-0.49 \pm 0.25$, $-0.59 \pm 0.13$, $-0.62 \pm 0.19$, and $-0.75 \pm 0.07$ pA at −60, −70, −80, −90, and −100 mV, respectively, giving a conductance of 7.6 pS. Channel openings of CsCl-exposed patches had mean amplitudes of $-0.44 \pm 0.03$, $-0.50 \pm 0.04$, $-0.55 \pm 0.05$, $-0.63 \pm 0.08$, $-0.73 \pm 0.03$, $-0.82 \pm 0.05$ and $0.99 \pm 0.04$ pA at −50, −60, −70, −80, −90, −100 and −120 mV, respectively, giving a conductance of 8.0 pS (Gaussian mean ± S.D.; slope conductance by linear regression, $r = 0.99$ and 0.995).

not appear to affect the peak control fractional activation (DiFrancesco & Mangoni, 1994; Michels *et al.* 2005); therefore, we tentatively assumed that $P_o$ would plateau near the peak control $P_o$ (0.8) and estimated a $V_{1/2}$ of $-76.6 \pm 2.5$ mV with slope $-7.8 \pm 2.2$ mV (Boltzmann fit ± S.E.M.). However, if the peak $P_o$ increased towards 1, this $V_{1/2}$ would hyperpolarize. Similar to control values, the extrapolated reversal potential, slope conductance, and

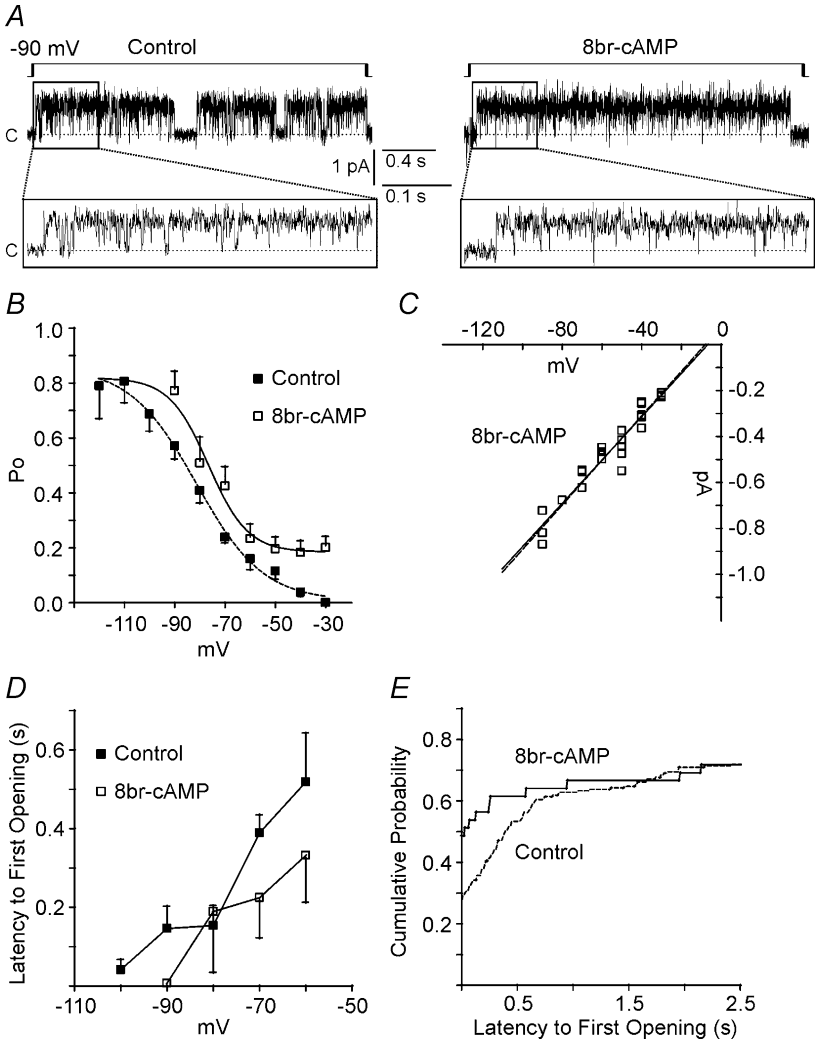


**Figure 4. cAMP increases open probabilities, decreases first-latencies and does not effect conductance of single h-channels**

*A*, representative traces of channel openings elicited by hyperpolarization steps from −30 mV to −90 mV in control and 10 $\mu$M 8Br-cAMP conditions. Based on inside-out patch configuration, positive (upward) deflections represent inward current. Closed state is indicated by c and dashed line. *B*, 8Br-cAMP (10 $\mu$M) increased $P_o$ values, but every patch was lost by −90 mV. Therefore, we assumed that the peak $P_o$ would be near the control peak (0.8) by −120 mV and fitted the data with a Boltzmann equation resulting in $V_{1/2}$ of $-76.6 \pm 2.5$ mV and slope $-7.8 \pm 2.2$ mV ($n = 12$–70 sweeps from 2 to 6 patches). The control $V_{1/2}$ was $-81.3 \pm 1.8$ mV and slope $-13.3 \pm 1.9$ mV (dashed line). *C*, similar to control, 10 $\mu$M 8Br-cAMP-exposed channels had a slope conductance of 9.4 pS. Dashed line is the control *I–V* fit from Fig. 2*B*. Voltages and current amplitudes are corrected for patch configuration. The Gaussian-fit histograms of pooled events from all 8Br-cAMP patches (not shown) resulted in current amplitudes of $-0.21 \pm 0.07$, $-0.30 \pm 0.09$, $-0.43 \pm 0.06$, $-0.44 \pm 0.04$, $-0.54 \pm 0.06$, $-0.65 \pm 0.02$, and $-0.79 \pm 0.03$ pA at −30, −40, −50, −60, −70, −80 and −90, mV, respectively, giving a conductance of 9.1 pS (Gaussian mean ± S.D.; slope conductance by linear regression, $r = 0.99$; $P > 0.05$ *versus* control (Fig. 2 legend) by unpaired *t* test). *D*, averaged latencies to first channel openings after a voltage step decreased with hyperpolarization, but were not decreased significantly by 10 $\mu$M 8Br-cAMP ($P > 0.05$ *versus* control by unpaired *t* test). Only steps activating channels were included (control, $n = 35$–151 sweeps from 5 to 8 patches; 8Br-cAMP, $n = 12$–29 sweeps from 2 to 6 patches). *E*, cumulative frequency distribution histograms of the latency to first channel openings during a −70 mV step demonstrated 8Br-cAMP increased probabilities of first openings for latencies ≤ 1 s, but did not modulate cumulative probabilities of latencies ≥ 1 s (bin width = 10 ms). Sweeps with no channel openings were included (control, $n = 201$ sweeps from 8 patches; 8Br-cAMP, $n = 39$ sweeps from 4 patches).

**Table 2. Control and 8br-cAMP open time constants**

| mV | $\tau_{long}$ (ms) | $A_{long}$ | $\tau_{short}$ (ms) | $A_{short}$ | $r$ | $n$ | events |
|---|---|---|---|---|---|---|---|
| Control | | | | | | | |
| −60 | 5.8 | 66% | 1.8 | 34% | 0.97 | 6 | 8768 |
| −70 | 10.5 | 39% | 2.3 | 61% | 0.97 | 8 | 17353 |
| −80 | 16.8 | 12% | 3.2 | 88% | 0.96 | 8 | 5350 |
| −90 | 19.3 | 23% | 3.0 | 77% | 0.91 | 6 | 3924 |
| −100 | 30.0 | 12% | 3.2 | 88% | 0.91 | 5 | 2052 |
| 8Br-cAMP | | | | | | | |
| −30 | 85.2 | 9% | 18.6 | 91% | 0.68 | 3 | 858 |
| −40 | 26.7 | 32% | 9.5 | 68% | 0.75 | 4 | 748 |
| −50 | 43.5 | 36% | 10.3 | 64% | 0.63 | 3 | 416 |
| −60 | 44.3* | 25%* | 6.0* | 75%* | 0.71 | 6 | 673 |
| −70 | 27.2* | 24%* | 5.2* | 76%* | 0.90 | 4 | 2009 |
| −80 | n.d. | | n.d. | | | | |
| −90 | n.d. | | n.d. | | | | |

Open times were calculated from standard exponential fits of distribution histograms (bin width = 1 ms). Abbreviations: $\tau$, time constant; $A$, area that $\tau_{long}$ or $\tau_{short}$ contributes to the exponential fit; $r$, correlation coefficient of exponential fit; $n$, number of patches; n.d., not determined. Voltages corrected for patch configuration. Significance was determined with unpaired $t$ tests. *$P \leq 0.001$ *versus* control patches.

apparent $P_{Na}/P_K$ of channels exposed to 8Br-cAMP were −6.7 mV, 9.4 pS and 0.81 (Fig. 4*C*).

The mean latencies to first channel opening remained voltage dependent, but were not significantly decreased by 8Br-cAMP (Fig. 4*D*). However, cumulative distribution histograms revealed that 8Br-cAMP increased the probability of a first channel opening for latencies $\leq 1$ s after the voltage step, but cumulative probabilities were similar to control for latencies $\geq 1$ s (Fig. 4*E*). Channel open times (long and short) were also increased by 8Br-cAMP and appeared to decrease with hyperpolarization (Table 2).

## Discussion

This study presents the first evidence of *neuronal* unitary conductances with properties of single h-channels. These unitary currents: (1) activated upon membrane hyperpolarization; (2) had voltage-dependent characteristics similar to macroscopic $I_h$; (3) were non-inactivating; and (4) were modulated by compounds known to act on macroscopic $I_h$. Together, these data provide compelling evidence for the HCN channel identity of the unitary currents described.

### Properties of novel single channels

Unitary currents recorded from CA1 pyramidal cells were elicited by hyperpolarization. The apparent threshold for channel activation was between −50 and −70 mV depending on individual patches. Channel open probabilities and open times increased upon progressive hyperpolarization. The $V_{1/2}$ of channel open probabilities was −81 mV (Fig. 2*A*), similar to the $V_{1/2}$ of activation of macroscopic $I_h$ in CA1 pyramidal cells (Vasilyev & Barish, 2002; van Welie *et al.* 2004). In addition, the latency to the first channel opening was modulated by voltage, decreasing 12-fold between −60 and −100 mV. Furthermore, the ensemble averaged current was non-inactivating with an activation time constant very similar to activation time constants of macroscopic $I_h$ of CA1 pyramidal neurones (Vasilyev & Barish, 2002; van Welie *et al.* 2004) and macroscopic currents of expressed HCN1 channels (Chen *et al.* 2001; Altomare *et al.* 2003). These observations support the h-channel identity of the recorded conductances.

Interestingly, the values of open probability and $V_{1/2}$ found in patches from CA1 pyramidal cells were higher and more depolarized, respectively, than those reported for macroscopic $I_h$ of inside-out patches from heterologous systems or other tissues. Thus, macroscopic $I_h$ of patches from oocytes, expressing either HCN1 or HCN2 channels, and sinoatrial cells had $V_{1/2}$ values that were negatively shifted by at least 30 mV compared to the whole cell configuration, predicting low open probabilities at voltages more positive than −100 mV (DiFrancesco & Mangoni, 1994; Chen *et al.* 2001). This shift was partially attributable to the loss of intracellular cAMP in the inside-out configuration. Here, our inside-out patch $V_{1/2}$ value resembles those found in whole-cell studies (Vasilyev & Barish, 2002; van Welie *et al.* 2004). This preservation of $V_{1/2}$ characteristics may derive from intrinsic differences between *neuronal* membranes and oocyte or sinoatrial cell membranes. For example, interaction of the neuronal h-channels with putative $\beta$ subunits (e.g. minK-related protein-1; Yu *et al.* 2001; Proenza *et al.* 2002; Altomare *et al.* 2003; Qu *et al.* 2004), scaffolding proteins (Gravante *et al.* 2004; Kimura *et al.* 2004) or cytoskeletal proteins (Santoro *et al.* 2004), possibly preserved in our neuronal preparations, might support a more 'native' gating of the channels.

The equilibrium potential (−8.1 mV) and apparent $P_{Na}/P_K$ (0.76) of these single-channel currents were similar, but not identical, to macroscopic $I_h$ (Accili *et al.* 2002; Robinson & Siegelbaum, 2003). Interestingly, retrospective examination of the sinoatrial inside-out patch single h-channel study (DiFrancesco & Mangoni, 1994) revealed a similarity to the current findings: calculating $P_{Na}/P_K$ using the values from the DiFrancesco & Mangoni (1994) study yielded an apparent $P_{Na}/P_K$ value of 0.91, comparable to the value reported here. The basis for the divergent $P_{Na}/P_K$ ratios between inside-out and cell-attached or whole-cell patch configurations is not yet clear. However, these values are only estimates since ionic substitution experiments were not performed in either study.

### Modulation of unitary currents

Macroscopic $I_h$ is sensitive to inhibition by ZD7288 and $Cs^+$ and enhancement by cAMP; thus, if the unitary currents recorded here are h-channels, they should be sensitive to these compounds. We chose relatively high concentrations of the blockers to obtain clear effects: for macroscopic $I_h$, 50 $\mu$M of ZD7288 blocks ~70% of the current, whereas 1 mM CsCl blocks > 50% of $I_h$ depending on cell type (Accili *et al.* 2002; Robinson & Siegelbaum, 2003). Consistent with their putative identity, single h-channels were markedly influenced by these compounds: ZD7288 and CsCl slightly decreased channel conductance, greatly reduced $P_o$, increased latencies to first openings, and decreased the short and long open times, whereas 8Br-cAMP increased $P_o$, depolarized the $V_{1/2}$ by $\leq$ 4.7 mV, decreased latencies to first channel openings, prolonged open times, but did not affect channel conductance. These modulations are likely to account for the positive and negative effects of the compounds on macroscopic $I_h$. Taken together, the effects of ZD7288, CsCl and 8Br-cAMP on the unitary conductances support their h-channel identity.

Interestingly, the ZD7288 effects on single HCN channels found here are similar to predictions of ZD7288 effects on macroscopic $I_h$: Shin *et al.* (2001) determined that ZD7288 enters the HCN channel pore from the intracellular side, and suggested that it blocks either one open state and one closed state or two open states of the channel. Our data on unitary channels support the existence of at least two open states that may be influenced by ZD7288. Similarly, the effects of CsCl on single h-channels are consistent with expectations. CsCl blocks single channel currents of several voltage-gated $K^+$ ($K_v$) channels by decreasing mean open times (Fukushima, 1982; Sakmann & Trube, 1984); and because HCN channels are part of the $K_v$ channel 'superfamily' (Robinson & Siegelbaum, 2003), it is not surprising that $Cs^+$ also decreases open times of single h-channels.

HCN subunits contain a cyclic nucleotide-binding domain (CNBD) in their intracellular carboxy terminus which tonically inhibits gating. Binding of cAMP relieves this inhibition and shifts gating to more depolarized potentials (Robinson & Siegelbaum, 2003). This predicts that cAMP will not affect unitary conductance, but will increase $P_o$, as was found by DiFrancesco & Mangoni (1994). Our experiments replicate this finding and indicate that cAMP prolongs the duration of the open states.

### Previous studies

Two groups have described unitary h-channels recorded from sinoatrial node and myocyte cells, respectively, of the heart (DiFrancesco, 1986; DiFrancesco & Mangoni, 1994; Michels *et al.* 2005). DiFrancesco's group (1986, 1994), using both cell-attached and inside-out patch recording configurations, reported unitary current amplitudes of less than 0.15 pA with a conductance of ~1 pS. Recently, Michels *et al.* (2005), recorded single-channel $I_h$ from human atrial myocytes, with a conductance of 19 pS. This group also recorded unitary HCN1, HCN2 and HCN4 channels expressed in CHO cells, observing conductances of 12.9, 34.6 and 17.4 pS, respectively, well in line with our findings in hippocampal neurones. In contrast, Magee (1998) published a rigorous study on cell-attached somatic and dendritic patches where $I_h$ amplitudes were within the range of our single h-channel amplitudes and those of Michels *et al.* (2005), but reportedly did not observe unitary currents. An explanation for this discrepancy is unclear, but may stem from the different cell preparations (i.e. Magee used cells in intact slices), patch configuration (i.e. cell-attached *versus* inside-out) or acquisition and/or filtering rates. Possibly, the recording noise level may have obscured the discreet unitary events. Interestingly, based on our measured single h-channel properties and on values either from Vasilyev & Barish (2002) or from Magee (1998), estimates of h-channel densities of soma–proximal dendrites were very similar (i.e. ~0.04 and ~0.1 channels $\mu m^{-2}$). The same was found for distal dendrites (~0.4 and ~1 channels $\mu m^{-2}$). Thus, conductances of unitary h-channels seem to depend on both the subunit composition of the channel and the cell type recorded (i.e. CA1 pyramidal cells express HCN1 and HCN2, whereas atrial sinonode cells and myocytes express HCN2 and HCN4; Accili *et al.* 2002; Robinson & Siegelbaum, 2003).

In summary, this is the first report of native unitary $I_h$ in hippocampal neurones. Individual hippocampal cells express more than one HCN channel isoform, potentially resulting in mixed populations of homomeric and perhaps heteromeric channels (Santoro *et al.* 2000; Brewster *et al.* 2002). In addition, the formation of heteromultimeric h-channels may be dynamically regulated in normal and pathological states (Brewster *et al.* 2005). Isolation of single h-channels should enable identification of specific differences between homomeric and heteromeric channels and discovery of selective blockers that may be useful for neuropathological disorders.

## References

Accili EA, Proenza C, Baruscotti M & DiFrancesco D (2002). From funny current to HCN channels: 20 years of excitation. *News Physiol Sci* **17**, 32–37.

Altomare C, Terragni B, Brioschi C, Milanesi R, Pagliuca C, Viscomi C *et al.* (2003). Heteromeric HCN1-HCN4 channels: a comparison with native pacemaker channels from the rabbit sinoatrial node. *J Physiol* **549**, 347–359.

Beaumont V & Zucker RS (2000). Enhancement of synaptic transmission by cyclic AMP modulation of presynaptic Ih channels. *Nat Neurosci* **3**, 133–141.

Bender RA, Brewster A, Santoro B, Ludwig A, Hofmann F, Biel M *et al.* (2001). Differential and age-dependent expression of hyperpolarization-activated, cyclic nucleotide-gated cation channel isoforms 1–4 suggests evolving roles in the developing rat hippocampus. *Neuroscience* **106**, 689–698.

Brewster AL, Bender RA, Chen Y, Dube C, Eghbal-Ahmadi M & Baram TZ (2002). Developmental febrile seizures modulate hippocampal gene expression of hyperpolarization-activated channels in an isoform- and cell-specific manner. *J Neurosci* **22**, 4591–4599.

Brewster AL, Bernard JA, Gall CM & Baram TZ (2005). Formation of heteromeric hyperpolarization-activated cyclic nucleotide-gated (HCN) channels in the hippocampus is regulated by developmental seizures. *Neurobiol Dis* **19**, 200–207.

Chen S, Wang J & Siegelbaum SA (2001). Properties of hyperpolarization-activated pacemaker current defined by coassembly of HCN1 and HCN2 subunits and basal modulation by cyclic nucleotide. *J General Physiol* **117**, 491–504.

DiFrancesco D (1986). Characterization of single pacemaker channels in cardiac sino-atrial node cells. *Nature* **324**, 470–473.

DiFrancesco D & Mangoni M (1994). Modulation of single hyperpolarization-activated channels ($i_f$) by cAMP in the rabbit sino-atrial node. *J Physiol* **474**, 473–482.

Fukushima Y (1982). Blocking kinetics of the anomalous potassium rectifier of tunicate egg studied by single channel recording. *J Physiol* **331**, 311–331.

Gravante B, Barbuti A, Milanesi R, Zappi I, Viscomi C & DiFrancesco D (2004). Interaction of the pacemaker channel HCN1 with filamin A. *J Biol Chem* **279**, 43847–43853.

Hamill OP, Marty A, Neher E, Sakmann B & Sigworth FJ (1981). Improved patch-clamp techniques for high-resolution current recording from cells and cell-free membrane patches. *Pflugers Arch* **391**, 85–100.

Hille B (2001). *Ion Channels of Excitable Membranes*. Sinauer Associates, Inc., Sunderland, MA, USA.

Johnston D & Wu SMS (1995). *Foundations of Cellular Neurophysiology*. MIT Press, Cambridge, MA, USA.

Kay AR & Wong RKS (1986). Isolation of neurons suitable for patch-clamping from adult mammalian central nervous systems. *J Neurosci Meth* **16**, 227–238.

Kimura K, Kitano J, Nakajima Y & Nakanishi S (2004). Hyperpolarization-activated, cyclic nucleotide-gated HCN2 cation channel forms a protein assembly with multiple neuronal scaffold proteins in distinct modes of protein–protein interaction. *Genes Cells* **9**, 631–640.

Lupica CR, Bell JA, Hoffman AF & Watson PL (2001). Contribution of the hyperpolarization-activated current ($I_h$) to membrane potential and GABA release in hippocampal interneurons. *J Neurophysiol* **86**, 261–268.

Magee JC (1998). Dendritic hyperpolarization-activated currents modify the integrative properties of hippocampal CA1 pyramidal neurons. *J Neurosci* **18**, 7613–7624.

Magee JC (1999). Dendritic $I_h$ normalizes temporal summation in hippocampal CA1 neurons. *Nature Neurosci* **2**, 508–514.

Michels GErF, Khan I, Sudkamp M, Herzig S & Hoppe UC (2005). Single-channel properties support a potential contribution of hyperpolarization-activated cyclic nucleotide-gated channels and If to cardiac arrhythmias. *Circulation* **111**, 399–404.

Poolos NP (2004). The yin and yang of the h-channel and its role in epilepsy. *Epilepsy Curr* **4**, 3–6.

Proenza C, Angoli D, Agranovich E, Macri V & Accili EA (2002). Pacemaker channels produce an instantaneous current. *J Biol Chem* **277**, 5101–5109.

Qu J, Kryukova Y, Potapova IA, Doronin SV, Larsen M, Krishnamurthy G *et al.* (2004). MiRP1 modulates HCN2 channel expression and gating in cardiac myocytes. *J Biol Chem* **279**, 43497–43502.

Rho JM, Donevan SD & Rogawski MA (1996). Direct activation of GABAA receptors by barbiturates in cultured rat hippocampal neurons. *J Physiol* **497**, 509–522.

Robinson RB & Siegelbaum SA (2003). Hyperpolarization-activated cation currents: from molecules to physiological function. *Annu Rev Physiol* **65**, 453–480.

Sakmann B & Trube G (1984). Voltage-dependent inactivation of inward-rectifying single-channel currents in the guinea-pig heart cell membrane. *J Physiol* **347**, 659–683.

Santoro B & Baram TZ (2003). The multiple personalities of h-channels. *Trends Neurosci* **26**, 550–554.

Santoro B, Chen S, Luthi A, Pavlidis P, Shumyatsky GP, Tibbs GR, Siegelbaum SA (2000). Molecular and functional heterogeneity of hyperpolarization-activated pacemaker channels in the mouse CNS. *J Neurosci* **20**, 5264–5275.

Santoro B, Wainger BJ & Siegelbaum SA (2004). Regulation of HCN channel surface expression by a novel C-terminal protein–protein interaction. *J Neurosci* **24**, 10750–10762.

Shin KS, Rothberg BS & Yellen G (2001). Blocker state dependence and trapping in hyperpolarization-activated cation channels: evidence for an intracellular activation gate. *J General Physiol* **117**, 91–101.

Surges R, Freiman TM & Feuerstein TJ (2004). Input resistance is voltage dependent due to activation of Ih channels in rat CA1 pyramidal cells. *J Neurosci Res* **76**, 475–480.

Vasilyev DV & Barish ME (2002). Postnatal development of the hyperpolarization-activated excitatory current Ih in mouse hippocampal pyramidal neurons. *J Neurosci* **22**, 8992–9004.

van Welie I, van Hooft JA & Wadman WJ (2004). Homeostatic scaling of neuronal excitability by synaptic modulation of somatic hyperpolarization-activated Ih channels. *Proc Natl Acad Sci U S A* **101**, 5123–5128.

Yu H, Wu J, Potapova I, Wymore RT, Holmes B, Zuckerman J *et al.* (2001). MinK-related peptide 1: a beta subunit for the HCN ion channel subunit family enhances expression and speeds activation. *Circ Res* **88**, E84–E87.

## Acknowledgements

This work was supported by NIH NS 35439 (T.Z.B.), NS 045540 (T.A.S.) and K02 NS 044846 (J.M.R.).